Published in final edited form as:
Angew Chem Int Ed Engl. 2009 ; 48(10): 1792–1797. doi:10.1002/anie.200804558.

A Bistable Poly[2]catenane Forms Nanosuperstructures**

Mark A. Olson,
Department of Chemistry, Northwestern University 2145 Sheridan Road, Evanston, IL 60208 (USA)

Adam B. Braunschweig,
Department of Chemistry, Northwestern University 2145 Sheridan Road, Evanston, IL 60208 (USA)

Lei Fang,
Department of Chemistry, Northwestern University 2145 Sheridan Road, Evanston, IL 60208 (USA)

Taichi Ikeda,
Functional Modules Group, Organic Nanomaterials Center National Institute for Materials Science 1-1 Namiki, Tsukuba 305-0044 (Japan)

Rafal Klajn,
Department of Chemistry, Northwestern University 2145 Sheridan Road, Evanston, IL 60208 (USA)

Ali Trabolsi,
Department of Chemistry, Northwestern University 2145 Sheridan Road, Evanston, IL 60208 (USA)

Paul J. Wesson,
Department of Chemistry, Northwestern University 2145 Sheridan Road, Evanston, IL 60208 (USA)

Diego Benítez,
Department of Chemistry, Northwestern University 2145 Sheridan Road, Evanston, IL 60208 (USA)

Chad A. Mirkin,
Department of Chemistry, Northwestern University 2145 Sheridan Road, Evanston, IL 60208 (USA)

Bartosz A. Grzybowski*, and
Department of Chemistry, Northwestern University 2145 Sheridan Road, Evanston, IL 60208 (USA)

J. Fraser Stoddart*
Department of Chemistry, Northwestern University 2145 Sheridan Road, Evanston, IL 60208 (USA)

**We gratefully acknowledge FENA and MURI for funding support. R.K. was supported by the MRSEC program of the National Science Foundation (DMR-0520513) at the Materials Research Center of Northwestern University. A.B.B. was supported by an NIH Postdoctoral Fellowship (IF32CA136148-01).

*Fax: (+1) 847-491-1009, grzybor@northwestern.edu, stoddart@northwestern.edu, Homepage: http://dysa.northwestern.edu/index.dwt, http://stoddart.northwestern.edu.

Dedicated to David Reinhoudt on the occasion of his 65th birthday

Supporting information for this article is available on the WWW under http://dx.doi.org/10.1002/anie.200804558.

Keywords

molecular devices; molecular switches; polymers; self-assembly; template synthesis

The introduction of the mechanical bond[1] into chemical compounds has contributed significantly to the realization[2] of precise molecular architechtonic tuning capabilities previously unattainable at the molecular scale. The relative molecular motions (e.g., circumrotation, translation, etc.) displayed within mechanically interlocked compounds, such as catenanes and rotaxanes, has led, as a result of templation[3] during their synthesis, to the emergence of bistability[4] necessary for the operation of molecular switches and machines[2] with potential uses in molecular electronic devices (MEDs), and in nanoelectromechanical systems (NEMS) such as "mechanized" nanoparticles (MNPs)[5] for controlled drug delivery. In the context of MEDs alone, molecular switches in the form of bistable rotaxanes have been used[6] to pattern a 160-kbit molecular electronic memory at a density of 10^{11} bits per square centimeter in a two-terminal crossbar device that is smaller than the cross-section of a white blood cell.

Despite these achievements, the challenge remains to make these bistable, mechanically interlocked molecules not only readily accessible synthetically, but also to display materials processibility suitable for efficient device fabrication. Motivated by the emerging trends in materials chemistry, these highly programmable, mechanically interlocked compounds are now being incorporated into reticular networks[7] and polymeric scaffolds.[8] Mechanically interlocked polymeric scaffolds (MIPS), such as main-chain,[10] pendant,[11] and bridged[12] classes of polycatenanes, however, remain a formidable synthetic challenge. MIPS have long been known[7–12] to possess unique mechanical and dynamic properties. As a functional category of MIPS, mechanically interlocked switchable polymeric scaffolds[13] (MISPS) could benefit enormously from the combination of bistable molecular switchability and materials processibility.

Recent research[14] has uncovered efficient routes to synthesize the tetracationic cyclophane, namely $CBPQT^{4+}$, or cyclobis(paraquat-*p*-phenylene)-containing compounds, using the Cu^{I}-catalyzed Huisgen 1,3-dipolar cycloaddition[15] as the so-called click reaction.[16] These findings have enabled convenient and modular syntheses of the required complex molecules in high yields.[17] By incorporating a pendant alkyne group onto the π-electron deficient $CBPQT^{4+}$ ring, the click reaction can be used to graft this tetracationic cyclophane, and (bistable) [2]catenanes containing it, onto polymers carrying azide side-chains. Herein, we report the synthesis, actuation, ground-state equilibrium thermodynamics and switching kinetics of bistable poly[2]catenane-based nano-particles (NPs). These NPs give rise to hierarchical, self-assembled superstructures whose formation can be rationalized by electrostatic and surface effects.

The copper-catalyzed click reaction between azide and alkyne functions in polymeric materials is reported[18] to go to high conversion in part, it is believed, because of the increased solubility of the Cu^{I} species by the accumulating polytriazoles, which results in autocatalysis. The rates of click reactions involving alkynes added to azide-functionalized polymers have been shown[19] to be much faster than those using the corresponding monomer, most likely as a result of the anchimeric assistance. Starting with the side-chain azide-functionalized polymer **1** (M_w = 55 000 $gmol^{-1}$ and M_n = 39000 $gmol^{-1}$, PDI = 1.4), obtained by atom transfer radical polymerization (ATRP), 1) the bistable side-chain poly[2]-catenane co-polymer[20] **5**·*n*PF_6, and the control co-polymer,[20] and 2) the side-chain poly-$CBPQT^{4+}$ **4**·*n*PF_6 were obtained (Scheme 1) in ≥95% conversion, as determined by end-group analysis using ^{1}H NMR spectroscopy, and were isolated in 91 and 96%yields,

repectively. Assuming the click reaction proceeds with almost complete conversion and, based on the molar ratio of the azide functions to the alkyne-functionalized catenane **3**·4PF_6, a theoretical M_n of 128 000 $gmol^{-1}$ for **5**·*n*PF_6 was calculated; this value agrees with that estimated from end-group analysis by ^{1}H NMR spectroscopy. Analysis by size exclusion chromatography, coupled with detection by multi-angle light scattering (SEC-MALS), confirmed the aggregation behavior of **5**·*n*PF_6 in DMF with the calculated values for M_w of $(1.30 \pm 0.07) \times 10^6$ $gmol^{-1}$, M_n of $(8.70 \pm 0.61) \times 10^5$ $gmol^{-1}$, and a PDI of 1.5 ± 0.1, corresponding to an RMS radius of gyration (r_g) of 127(±2.5) nm for the nanoparticles. The SEC-MALS conformation plot of log r_g as a function of log M_w for **5**·*n*PF_6 yields a slope of 0.34 (±0.01), a value which is consistent[21] with spherical nanoparticles being present in solution (see Supporting Information for further details). Although SEC-MALS also reveals that **4**·*n*PF_6 aggregates strongly in solution, the conformation plots do not indicate the presence of any spherical nanoparticles in solution. In a series of independent measurements,[22] diffusion coefficients (D_0) of $(1.15 \pm 0.05) \times 10^{-12}$ m^2 s^{-1} for **5**·*n*PF_6 and $(1.51 \pm 0.06) \times 10^{-9}$ m^2 s^{-1} for **3**·4PF_6 were measured by double potential step chronocoulometry[23] (see Supporting Information) in DMF at 298 K and applying the Cottrell relationship.[24] Dynamic light scattering (DLS) measured a diffusion coefficient of $(2.22 \pm 0.21) \times 10^{-12}$ m^2 s^{-1} for **5**·*n*PF_6, and a hydrodynamic radius (R_h) of 174(±32) nm, yielding an R_g/R_h value of 0.730(±0.13)—again indicating[25] the pre-scence of spherical particles in solution. The [2]catenane and $CBPQT^{4+}$ side-chain functionalized polymers were further characterized (see Supporting Information) by ^{1}H NMR and ^{1}H-^{1}H g-DQF-COSY NMR spectroscopies.

Bistable [2]catenanes, based on the highly preferred encirclement of the tetrathiafulvalene (TTF) over dioxynaphthalene (DNP) units, both located in the macrocyclic polyethers, by the $CBPQT^{4+}$ ring have been investigated[26] extensively. Switching within these molecules can be initiated[26, 27] by either chemical or electrochemical stimuli. This switching manifests itself in the form of mechanical circumrotation of the macrocyclic polyether component with respect to the $CBPQT^{4+}$ ring. The bistability presents itself as an equilibrium between two translational isomers in which the ground-state co-conformation (GSCC) and the metastablestate co-conformation (MSCC) correspond to the encirclement within the macrocyclic polyethers of the TTF and DNP units, respectively, by the $CBPQT^{4+}$ ring. The ratio of GSCC to MSCC at 298 K is roughly 9:1, corresponding to a $\Delta G°$ value of 1.6 $kcalmol^{-1}$ when the $CBPQT^{4+}$ ring is free to circumrotate between the TTF and DNP units in bistable catenanes in solution.[28]

In solution, the thermochromic properties of both the **3**·4PF_6- and **5**·*n*PF_6-derived NPs were examined (Figure 1) by variable temperature (VT) UV/Vis spectroscopy in DMF in order to quantify the ground-state equilibrium thermodynamic parameters. The charge-transfer (CT) band situated at 812 nm is characteristic[26] of TTF residing inside $CBPQT^{4+}$ (GSCC), whereas DNP encircled by $CBPQT^{4+}$ (MSCC) produces a characteristic[26] CT band at 475 nm in DMF. Upon cooling the solution, the TTF/$CBPQT^{4+}$ CT band (ε = 4000 $Lmol^{-1}cm^{-1}$) increases in intensity while the DNP/$CBPQT^{4+}$ CT band decreases, indicating that the equilibrium between the translational isomers favors the GSCC at lower temperatures. Heating the solution produces the opposite trend, namely an increase in the intensity of the DNP/$CBPQT^{4+}$ CT band, accompanied by a decrease in the TTF/$CBPQT^{4+}$ CT band. In conjunction with VT ^{1}H NMR spectra recorded to determine the equilibrium constant for the GSCC/MSCC ratio in **3**·4PF_6 at 298 K, Van't Hoff plots were constructed in order to obtain the standard enthalpy ($\Delta H°$) and standard entropy ($\Delta S°$) for the equilibration (Table 1) of the GSCC with the MSCC. The GSCC→MSCC processes[29] in **3**·4PF_6 and **5**·*n*PF_6 correspond to $\Delta G°$ values of 1.5(±0.24) and 1.6(±0.05) $kcalmol^{-1}$, respectively.

Tetrathiafulvalene undergoes a sequential and reversible two-electron oxidation process ($TTF \rightarrow TTF^{\bullet+} \rightarrow TTF^{2+}$), generating cationic species, a property which triggers switching through circumrotation in **3**·*n*PF_6 and **5**·*n*PF_6 of the macrocyclic polyether with respect to the $CBPQT^{4+}$ ring. Reduction of these cationic species back to being neutral forms the MSCC which re-equilibrates to the equilibrium mixture of the GSCC and MSCC. Switching of the GSCC to the MSCC, which was achieved electrochemically,[30] was followed by cyclic voltammetry (CV), differential pulse voltammetry (DPV), and spectroelectrochemistry. In the case of the bistable poly[2]catenane **5**·*n*PF_6, the GSCC CT band at 812 nm bleaches (Figure 2 a) as the voltage is increased and new absorptions emerge at 445 and 595 nm for the $TTF^{\bullet+}$ radical cation. At voltages above 700 mV, the simultaneous disappearance of the peaks at 445 and 595 nm and the appearance of a DNP CT band at 520 nm indicates the oxidation of $TTF^{\bullet+}$ to TTF^{2+} dication. Similar spectral changes are observed (Figure 2b) by spectroelectrochemistry when **5**·*n*PF_6 is treated with 2 equivalents of $Fe(ClO_4)_3$. The TTF^{2+} dication, which is formed by this chemical oxidation, can be reduced back to a neutral TTF unit reversibly upon addition of aqueous ascorbic acid. These observations confirm that, even when the bistable [2]catenanes are attached to a polymer backbone and the poly[2]catenane assembles to give larger secondary superstructures, they can still operate as molecular switches under redox control (see the Supporting Information for CV measurements on **3**·4PF_6 and **5**·*n*PF_6). Following electromechanical actuation, recovery of the MSCC/GSCC equilibrium is an activated process. The kinetics of the relaxation of the MSCC back to the GSCC can be quantified by variable scan rate CV (Figure 3a) and fitting (Figure 3b) a first order decay model to the population ratios of the metastable state and the relaxation times. The role of the physical environment on molecular electromechanical switching in solution,[26, 28, 31] polymer gels,[29] self-assembled monolayers,[32] molecular switch tunnel junctions[27, 33] (MSTJs), and MEDs has already been probed[28, 34] in considerable detail. For **3**·4PF_6 and **5**·*n*PF_6, the $\Delta G^{\ddagger}$ values were found to be 17.8-(±5.0) and 17.4(±0.5) kcal mol^{-1}, respectively, in DMF. We conclude that the bistable [2]catenane side-chains in **5**·*n*PF_6 are equally accessible to solvent as in **3**·4PF_6, so both [2]catenanes experience very similar environments. Perhaps the appended [2]catenanes in **5**·*n*PF_6 reside on the peripheries of the secondary superstructures in solution.

The self-assembled superstructures of **5**·*n*PF_6 were examined (Figure 4a–d) by scanning electron microscopy (SEM). In a highly dilute solution of **5**·*n*PF_6 in MeCN the polymers assemble into hollow spherical shells (see inset in Figure 4b). The outer radii of these structures are around 200 nm that is, in agreement with the results from SEC-MALS, DLS, and chronocoulometry experiments. In the dry state, the particles appear flattened/collapsed with holes present on their surfaces. The formation of these nanoscopic superstructures (NS) can be rationalized based on the minimization of electrostatic[35] and surface energies[36] during the assembly of multiple (*n*) **5**·*n*PF_6 charged "globules" into one NS.

For both of these structures, the electrostatic energy can be expressed as

$$E_{\Phi,i}=\frac{1}{2}\int_V \rho_+ \Phi \mathrm{d}V$$

where ρ_+ is the charge density inside of the polymer, and the potential, Φ, is estimated using the Poisson equation,

$$\nabla^2\Phi=\frac{-\rho_+}{\varepsilon_0\varepsilon_\mathrm{p}}$$

for the polymer phase and the linearized form of the Poisson– Boltzmann equation,

$$\nabla^2\Phi=\kappa^2\Phi$$

for the surrounding solution (κ^{-1} is the Debye screening length, ε_0 is the permittivity of free space, and ε_p is the dielectric constant of the NS). The surface energy is calculated from $E_{\sigma,i} = \sigma A$, where σ is the surface tension of the polymer–solution interface and A is the surface area. Calculations detailed in the Supporting Information show that 1) the process of self-organization is indeed energetically favorable and 2) the dimensions of the NS can be found by minimizing the energetic change of this process per globule,

$$\frac{\Delta E}{n}=\frac{(E_{\Phi,\mathrm{NS}}+E_{\sigma,\mathrm{NS}})}{n}-E_{\Phi,\mathbf{5}\cdot n\mathrm{PF}_6}-E_{\sigma,\mathbf{5}\cdot n\mathrm{PF}_6},$$

with respect to the NS radius. Specifically, for an experimentally observed shell thickness of 20 nm, and for physically reasonable values of other parameters ($\varepsilon_p \approx 37$, $\sigma \approx 10$ m N m^{-1}, $\kappa^{-1} \approx 1.6$ nm, and $\rho_+ \approx 10^5$ Cm^{-3}), the model predicts an outer NS radius of 181 nm—that is, close to the experimental value. Finally, we observe that upon slow solvent evaporation on glass (Figure 4c,d), the polymeric NPs can form higher-level aggregates such as chains or joist-like chunks. Assembly of these structures is most likely driven by van der Waals forces that become increasingly important in the case of larger particles.

In summary, we have developed a highly efficient synthetic route to bistable side-chain poly[2]catenanes that self-assemble into novel types of supramolecular architectures including hollow spheres and their higher aggregates. These structures form as a result of a subtle interplay between electrostatic and surface forces acting as one in the system. A combination of analytical tools provides clear evidence that electromechanical switching of bistable [2]catenane units occurs in both free polymers and their nanoscopic assemblies. The maintenance of function in bistable mechanically interlocked units across ever-increasing levels of structural and superstructural complexity argues well for the emergence of mechanically interlocked switchable polymeric scaffolds, i.e., MISPS for use in molecular electronic devices.

Supplementary Material

Refer to Web version on PubMed Central for supplementary material.

References

1. Stoddart JF, Colquhoun HM. Tetrahedron. 2008; 64:8231–8263.
2. a) Balzani V, Credi A, Raymo FM, Stoddart JF. Angew. Chem. 2000; 112:3484–3530. *Angew. Chem. Int. Ed.* **2000**, *39*, 3348 – 3391; b) Collier JP, Heitz V, Sauvage JP. Top. Curr. Chem. 2005; 262:29–62.c) Braunschweig AB, Northrop BH, Stoddart JF. J. Mater. Chem. 2006; 16:32–44.d) Kay ER, Leigh DA, Zerbetto F. Angew. Chem. 2007; 119:72–196. *Angew. Chem. Int. Ed.* **2007**, *46*, 72 – 191; [PubMed: 17133632] e) Willner I, Basnar B, Willner B. Adv. Funct. Mater. 2007; 17:702–717.f) Balzani, V.; Credi, A.; Venturi, M. Molecular Devices and Machinery: Concepts and Perspectives for the Nanoworld. Wiley-VCH: Weinheim; 2008.
3. a) Busch DH, Stephenson NA. Coord. Chem. Rev. 1990; 100:119–154.b) Anderson HL, Anderson S, Sanders JKM. Acc. Chem. Res. 1993; 26:469–475.c) Diederich, F.; Stang, PJ., editors. Templated Organic Synthesis. Wiley-VCH: Weinheim; 2006. d) Stoddart JF, Tseng H-R. Proc. Natl. Acad. Sci. USA. 2002; 99:4797–4800. [PubMed: 11891314] e) Blanco MJ, Chambron JC,

Jiménez MC, Sauvage J-P. Top. Stereochem. 2003; 23:125–173.f) Busch DH. Top. Curr. Chem. 2005; 249:1–65.g) Griffiths KE, Stoddart JF. Pure Appl. Chem. 2008; 80:485–506.

4. Anelli P-L, Spencer N, Stoddart JF. J. Am. Chem. Soc. 1991; 113:5131–5133.b) Bissell RA, Cordova E, Kaifer AE, Stoddart JF. Nature. 1994; 369:133–137.c) Asakawa M, Ashton PR, Balzani V, Credi A, Hamers C, Mattersteig G, Montalti M, Shipway AN, Spencer N, Stoddart JF, Tolley MS, Venturi M, White AJP, Williams DJ. Angew. Chem. 1998; 110:357–361. *Angew. Chem. Int. Ed*. **1998**, *37*, 333–337; d) Aprahamian I, Yasuda T, Ikeda T, Saha S, Dichtel WR, Isoda K, Kato T, Stoddart JF. Angew. Chem. 2007; 119:4759–4763. *Angew. Chem. Int. Ed*. **2007**, *46*, 4675–4679.
5. Saha S, Leung KC-F, Nguyen TD, Stoddart JF, Zink JI. Adv. Funct. Mater. 2007; 17:685–693.
6. Green JE, Choi JW, Boukai A, Bunimovich Y, Johnston-Halperin E, DiIonno E, Luo Y, Sheriff BA, Xu K, Shin YS, Tseng H-R, Stoddart JF, Heath JR. Nature. 2007; 445:414–417. [PubMed: 17251976]
7. a) Tiburcio J, Davidson GJE, Loeb SJ. Chem. Commun. 2002:1282–1283.b) Yaghi OM, O'Keefe M, Ockwing NW, Chae HK, Eddaoudi M, Kim J. Nature. 2003; 423:705–715. and references therein; [PubMed: 12802325] c) Davidson GJE, Loeb SJ. Angew. Chem. 2003; 115:78–81. *Angew. Chem. Int. Ed*. **2003**, *42*, 74–77; d) Hoffart DJ, Loeb SJ. Angew. Chem. 2005; 117:923–926. *Angew. Chem. Int. Ed*. **2005**, *44*, 901–904; e) El-Kaderi HM, Hunt JR, Mendoza-Cortés JL, Côté AP, Taylor RE, O'Keefe M, Yaghi OM. Science. 2007; 316:268–272. [PubMed: 17431178] f) Banerjee R, Phan A, Wang B, Knobler C, Furukawa H, O'Keeffe M, Yaghi OM. Science. 2008; 319:939–943. [PubMed: 18276887]
8. Gibson HW, Nagvekar DS, Yamaguchi N, Bhattacharjee S, Wang H, Vergne MJ, Hercules DM. Macromolecules. 2004; 37:7514–7529.b) Zhang W, Dichtel WR, Stieg AZ, BenÍtez D, Gimzewski JK, Heath JR, Stoddart JF. Proc. Natl. Acad. Sci. USA. 2008; 105:6514–6519. [PubMed: 18448682]
9. a) Kern J-M, Sauvage J-P, Weidmann J-L. Tetrahedron. 1996; 52:10921–10934.b) Schwanke F, Safarowsky O, Heim C, Silva G, Vögtle F. Helv. Chim. Acta. 2000; 83:3279–3290.c) Amabilino DB, Ashton PR, Boyd SE, Lee JY, Menzer S, Stoddart JF, Williams DJ. Angew. Chem. 1997; 109:2160–2162. *Angew. Chem. Int. Ed. Engl*. **1997**, *36*, 2070–2072; d) Weizmann Y, Braunschweig AB, Wilner OI, Cheglakov Z, Willner I. Proc. Natl. Acad. Sci. USA. 2008; 105:5289–5294. [PubMed: 18391204]
10. a) Hamers C, Raymo FM, Stoddart JF. Eur. J. Org. Chem. 1998:2109–2117.b) Simone DL, Swager TM. J. Am. Chem. Soc. 2000; 122:9300–9301.
11. a) Weidmann J-L, Kern J-M, Sauvage J-P, Geerts Y, Muscat D, Müllen K. Chem. Commun. 1996:1243–1244.b) Menzer S, White AJP, Williams DJ, Bělohradský M, Hamers C, Raymo FM, Shipway AN, Stoddart JF. Macromolecules. 1998; 31:295–307.c) Muscat D, Köhler W, Räder HJ, Martin K, Mullins S, Müller B, Müllen K, Geerts Y. Macromolecules. 1999; 32:1737–1745.d) Weidmann J-L, Kern J-M, Sauvage J-P, Muscat D, Mullins S, Köhler W, Rosenauer C, Räder HJ, Martin K, Geerts Y. Chem. Eur. J. 1999; 5:1841–1851.e) Watanabe N, Ikari Y, Kihara N, Takata T. Macromolecules. 2004; 37:6663–6666.
12. a) Gibson HW, Bheda MC, Engen PT. Prog. Polym. Sci. 1994; 19:843–945.b) Godt A. Eur. J. Org. Chem. 2004:1639–1654.
13. Mechanically interlocked switchable polymeric scaffolds (MISPS) can be defined as a sub-category of MIPS in which the polymeric scaffolds are of oligomeric nature and larger, and contain and/or comprise one or many reversibly switchable (i.e., bistable, tristable, etc.) mechanically interlocked components. The definition includes both homo- and hetero-polyrotaxanes of both main-chain and side-chain classes as well as polycatenanes of main-chain, necklace, pendant, bridged, and side-chain classes. A switchable bistable catenane (or rotaxane) under this definition must undergo molecular mechanical motion (i.e., circumrotation, translation) between two states, generating isomeric species. Switching is usually initiated by an external stimulus, i.e., electrochemical, pH, light, temperature, etc.
14. a) Dichtel WR, Miljanić OŠ, Spruell JM, Heath JR, Stoddart JF. J. Am. Chem. Soc. 2006; 128:10388–10390. [PubMed: 16895403] b) Miljanić OŠ, Dichtel WR, Mortezaei S, Stoddart JF. Org. Lett. 2006; 8:4835–4838. [PubMed: 17020315]
15. a) Huisgen R. Pure Appl. Chem. 1989; 61:613–628.b) Huisgen R, Szeimies G, Möbuis L. Chem. Ber. 1967; 100:2494–2507.c) Bastide J, Hamelin J, Texier F, Ven VQ. Bull. Chim. Soc. Fr. 1973:2555–2579.Bastide J, Hamelin J, Texier F, Ven VQ. Bull. Chim. Soc. Fr. 1973:2871–2887.

16. a) Kolb HC, Finn MG, Sharpless KB. Angew. Chem. 2001; 113:2056–2075. *Angew. Chem. Int. Ed*. **2001**, *40*, 2004–2021. b) Rostovtsev VV, Green LG, Folkin VV, Sharpless KB. Angew. Chem. 2002; 114:2708–2711. *Angew. Chem. Int. Ed*. **2002**, *41*, 2596–2599.

17. a) Braunschweig AB, Dichtel WR, Miljanić OŠ, Olson MA, Spruell JM, Khan SI, Heath JR, Stoddart JF. Chem. Asian J. 2007; 2:634–647. [PubMed: 17465409] b) Aprahamian I, Dichtel WR, Ikeda T, Heath JR, Stoddart JF. Org. Lett. 2007; 9:1287–1290. [PubMed: 17326646]

18. Chan TR, Hilgraf R, Sharpless KB, Fokin VV. Org. Lett. 2004; 6:2853–2855. [PubMed: 15330631]

19. a) Sumerlin BS, Tsarevsky NV, Louche G, Lee RY, Matyjaszewski K. Macromolecules. 2005; 38:7540–7545.b) Tsarevsky NV, Sumerlin BS, Matyjaszewski K. Macromolecules. 2005; 38:3558–3561.c) Gao H, Matyjaszewski K. J. Am. Chem. Soc. 2007; 129:6633–6639. [PubMed: 17465551] d) Zhang J, Zhou Y, Zhu Z, Ge Z, Liu S. Macromolecules. 2008; 41:1444–1454.

20. Following the functionalization of polymer **1** with both 17%and 27% of the alkyne-derivatized tetracationic cyclophane and the [2]catenane, respectively, excess of methyl propargyl ether was attached onto the remaining free azide side-chains as a capping agent to generate random co-polymer products, namely **4**·*n*PF_6 and **5**·*n*PF_6 with no free azide moieties remaining. The use of the triethyleneglycol side-chain was designed to increase the solubility of **4**·*n*PF_6 and **5**·*n*PF_6.

21. a) Wyatt PJ. Anal. Chim. Acta. 1993; 272:1–40.b) Wu, C., editor. Handbook of Size Exclusion Chromatography and Related Techniques. New York: Marcel Dekker; 2004.

22. The use of pulsed field gradient NMR techniques to determine diffusion coefficients (D_0) of **5**·*n*PF_6 was avoided because of the extremely complicated ^{1}H NMR spectra that are characteristic of high molecular weight polymers containing a large number of dynamic mechanically interlocked entities. Dynamic light scattering is a much better alternative technique for measuring D_0 in **5**·*n*PF_6.

23. a) Ronconi CM, Stoddart JF, Balzani V, Baroncini M, Ceroni P, Giansante C, Venturi M. Chem. Eur. J. 2008; 14:8365–8373. [PubMed: 18666286] b) Yanez C, Basquinzay R. J. Electroanal. Chem. 2008; 622:242–245.

24. Bard, AJ.; Faulkner, LR. Electrochemical Methods: Fundamentals and Applications. Hoboken: Wiley; 2001.

25. a) Burchard W. Adv. Polym. Sci. 1983; 48:1–124.b) Israelachvili, JN. Intermolecular and Surface Forces. London: Academic Press; 1992. c) Kokufuta E, Ogawa K, Doi R, Kikuchi R, Farinato RS. J. Phys. Chem. B. 2007; 111:8634–8640. [PubMed: 17559254]

26. a) Balzani V, Credi A, Mattersteig GM, Matthews OA, Raymo FM, Stoddart JF, Venturi M, White AJP, Williams DJ. J. Org. Chem. 2000; 65:1924–1936. [PubMed: 10774011] b) Ikeda T, Saha S, Aprahamian I, Leung KC-F, Williams A, Deng W-Q, Flood AH, Goddard WA III, Stoddart JF. Chem. Asian J. 2007; 2:76–93. [PubMed: 17441141]

27. a) Collier CP, Mattersteig G, Wong EW, Luo Y, Beverly K, Sampaio J, Raymo FM, Stoddart JF, Heath JR. Science. 2000; 289:1172–1175. [PubMed: 10947980] b) Choi JW, Flood AH, Steuerman DW, Nygaard S, Braunschweig AB, Moonen NNP, Laursen BW, Luo Y, Delonno E, Peters AJ, Jeppesen JO, Xe K, Stoddart JF, Heath JR. Chem. Eur. J. 2006; 12:261–279. [PubMed: 16320367]

28. Steuerman DW, Tseng H-R, Peters AJ, Flood AH, Jeppesen JO, Nielsen KA, Stoddart JF, Heath JR. Angew. Chem. 2004; 116:6648–6653. *Angew. Chem. Int. Ed*. **2004**, *43*, 6486–6491.

29. a) Jeppesen JO, Nielsen KA, Perkins J, Vignon SA, Di Fabio A, Ballardini R, Gandolfi MT, Venturi M, Balzani V, Becher J, Stoddart JF. Chem. Eur. J. 2003; 9:2982–3007.b) Nygaard S, Leung KC-F, Aprahamian I, Ikeda T, Saha S, Laursen BW, Kim S-Y, Hansen SW, Stein PC, Flood AH, Stoddart JF, Jeppesen JO. J. Am. Chem. Soc. 2007; 129:960–970. [PubMed: 17243833]

30. Bilewicz R, Korybut-Daszkiewicz B, Rogowska A, Szydłowska J, Wieckowska A, Domagała S, Woźniak K. Electroanalysis. 2005; 17:1463–1470.

31. a) Asakawa M, Higuchi M, Mattersteig G, Nakamura T, Pease AR, Raymo FM, Shimizu T, Stoddart JF. Adv. Mater. 2000; 12:1099–1102.b) Bryce MR, Cooke G, Duclairoir FMA, John P, Perepichka DF, Polwart N, Rotello VM, Stoddart JF, Tseng H-R. J. Mater. Chem. 2003; 13:2111–2117.c) Tseng H-R, Wu D, Fang NX, Zhang X, Stoddart JF. ChemPhysChem. 2004; 5:111–116. [PubMed: 14999851] d) Bunker BC, Huber DL, Kushmerick JG, Dunbar T, Kelly M, Marzke C,

Cao J, Jeppesen JO, Perkins J, Flood AH, Stoddart JF. Langmuir. 2007; 23:31–34. [PubMed: 17190481]

32. Wong EW, Collier CP, Běhloradský M, Raymo FM, Stoddart JF, Heath JR. J. Am. Chem. Soc. 2000; 122:5831–5840.
33. Flood AH, Peters AJ, Vignon SA, Steuerman DW, Tseng H-R, Kang S, Heath JR, Stoddart JF. Chem. Eur. J. 2004; 10:6558–6564. [PubMed: 15562404]
34. Ciferri, A., editor. Supramolecular Polymers. New York: Marcel Dekker; 2000.
35. a) Kalsin A, Fialkowski M, Paszewski M, Smoukov SK, Bishop KJM, Grzybowski BA. Science. 2006; 312:420–424. [PubMed: 16497885] b) Bishop KJM, Grzybowski BA. ChemPhysChem. 2007; 8:2171–2176. [PubMed: 17763505]
36. Fialkowski M, Bitner A, Grzybowski BA. Nat. Mater. 2005; 4:93–97.

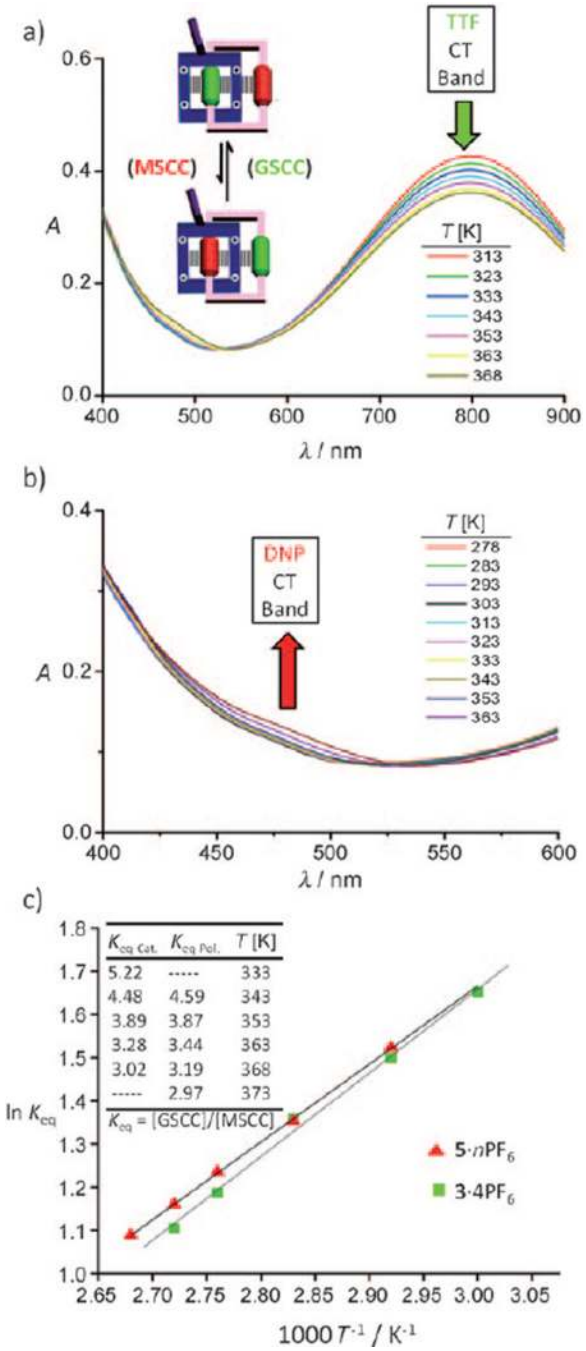

Figure 1.

a) Variable temperature UV/Vis spectra of the alkyne-functionalized [2]catenane **3**·4PF_6 and b) the side-chain poly[2]catenane **5**·*n*PF_6 (2×10^{-4} M, DMF) illustrating the temperature-dependent equilibrium (inset) between the GSCC (TTF-$CBPQT^{4+}$ charge-transfer band at 800 nm) and MSCC (DNP-$CBPQT^{4+}$ charge-transfer band at 480 nm). c) Linear Van't Hoff plots for **3**·4PF_6 ($R^2 = 0.996$) and **5**·*n*PF_6 ($R^2 = 0.996$) for the thermally induced GSCC→MSCC equilibrium change (inset); the ΔG°_{298K}, $\Delta H°$, and $\Delta S°$ values for the process were obtained as described in the footnotes to Table 1.

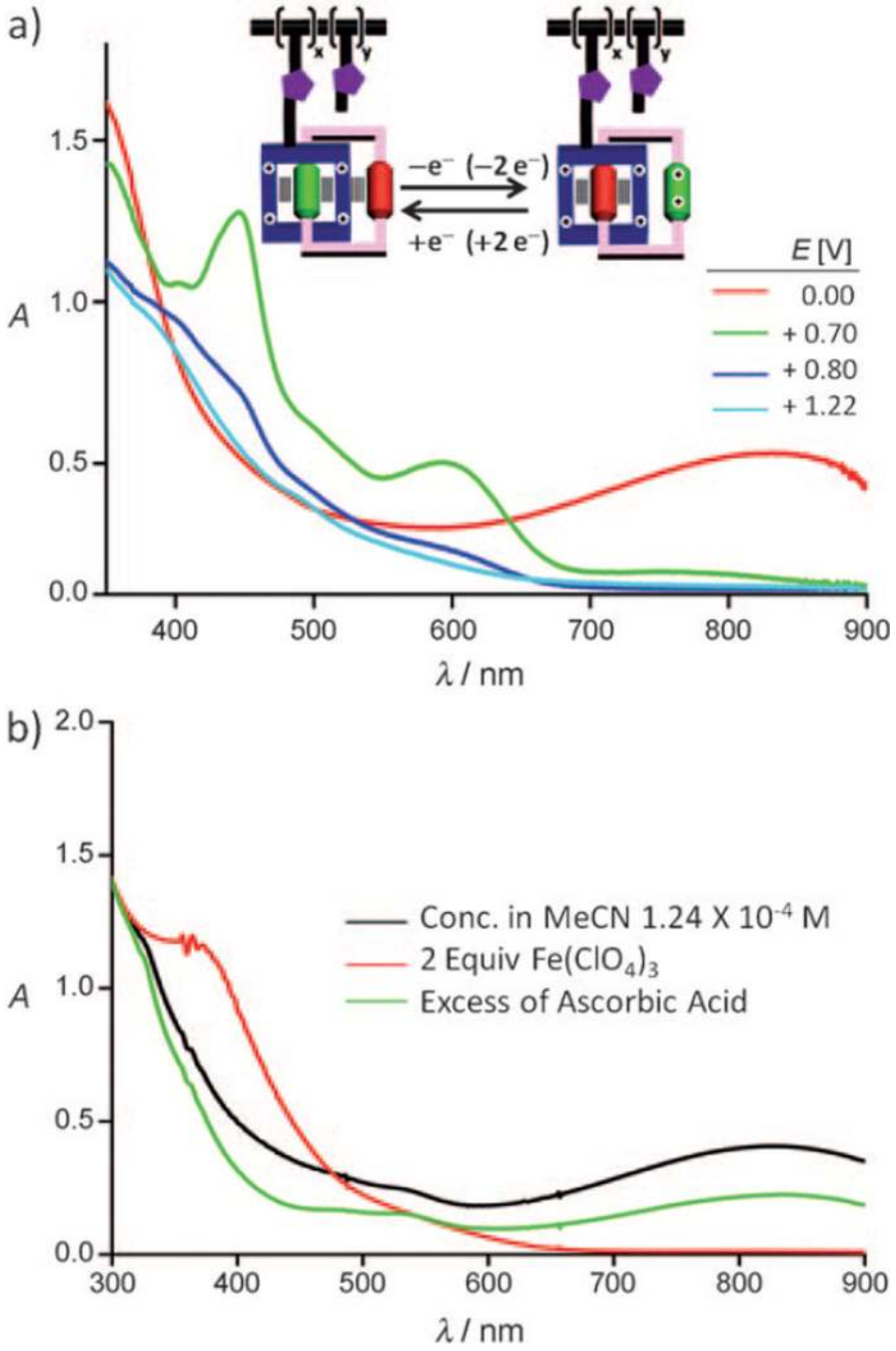

Figure 2.

a) UV/Vis spectroelectrochemistry of the bistable poly[2]catenane **5**·*n*PF_6 (5×10^{-4} M, MeCN, 0.1 M $TBAPF_6$, 298 K) recorded over a range of potentials illustrating the reversible two-electron electrochemically induced switching behavior of the bistable [2]catenane polymer side chains (inset). b) UV/Vis absorption spectra of the bistable poly[2]catenane **5** ·*n*PF_6 (1.24×10^{-4} M, MeCN, 298 K) illustrating the reversible chemically induced switching after the addition of 2 equivalents of the chemical oxidant $Fe(ClO_4)_3$ and reduction with an excess of ascorbic acid.

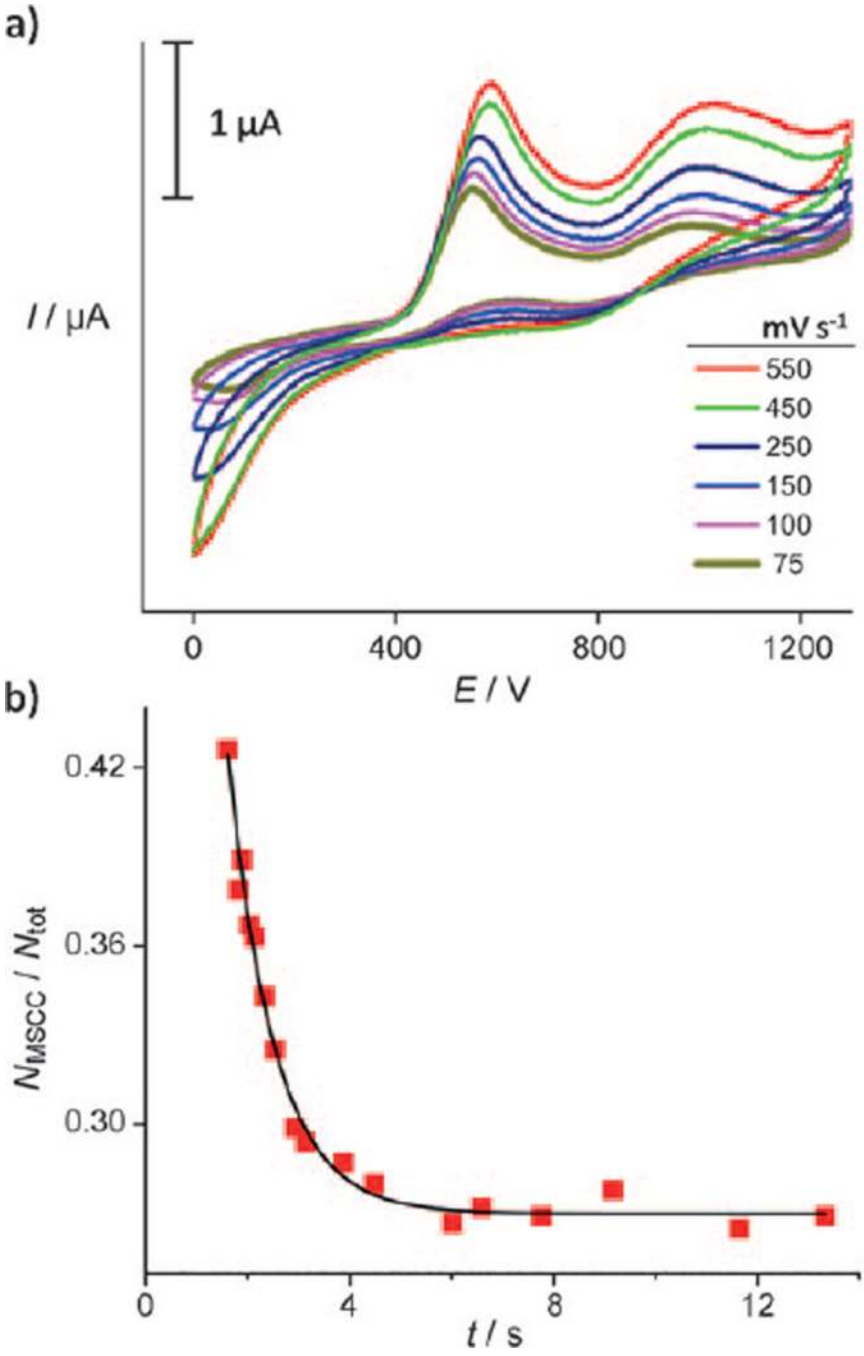

Figure 3.

a) Series of second cycle CVs for **5**·*n*PF_6 taken at varying scan rates (75/550 mVs^{-1}; 1 M $TBAPF_6$/298 K/DMF/versus Ag/AgCl). b) Fitting of a first-order decay model to the population ratios of the metastable state and relaxation times.

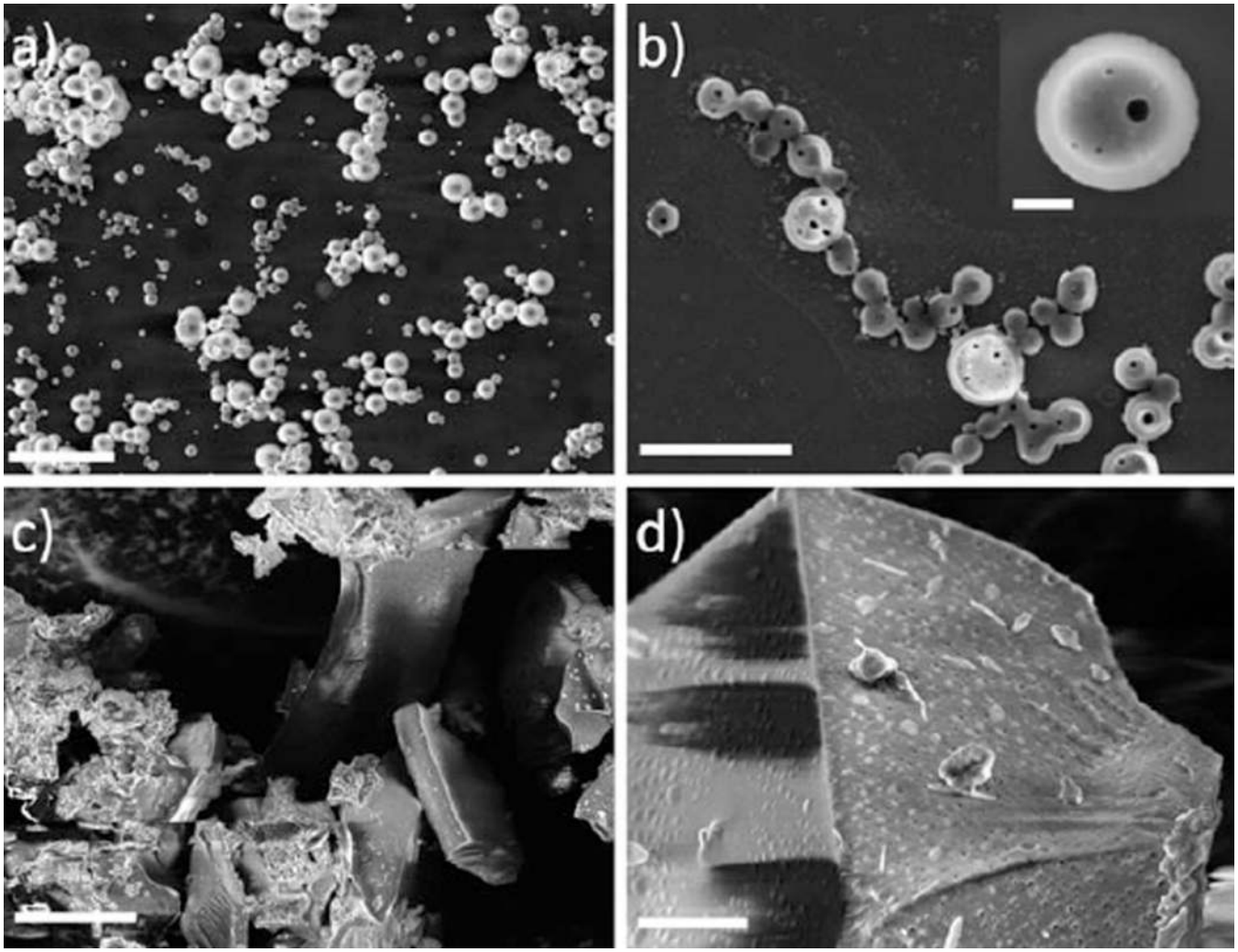

Figure 4.

a,b) SEM images of hollow polymer nanosized superstructures prepared by drop-casting a dilute solution of **5**·*n*PF_6, followed by removal of solvent under vacuum. SEM image (b, inset) of a single hollow polymer superstructure with clearly visible pores in the shell. c,d) SEM images of larger assembled superstructures prepared by slow solvent evaporation of **5**·*n*PF_6 on glass. The scale bars are a) 4 μm, b) 2 μm and 200 nm (inset), c) 20 μm, and d) 2 μm.

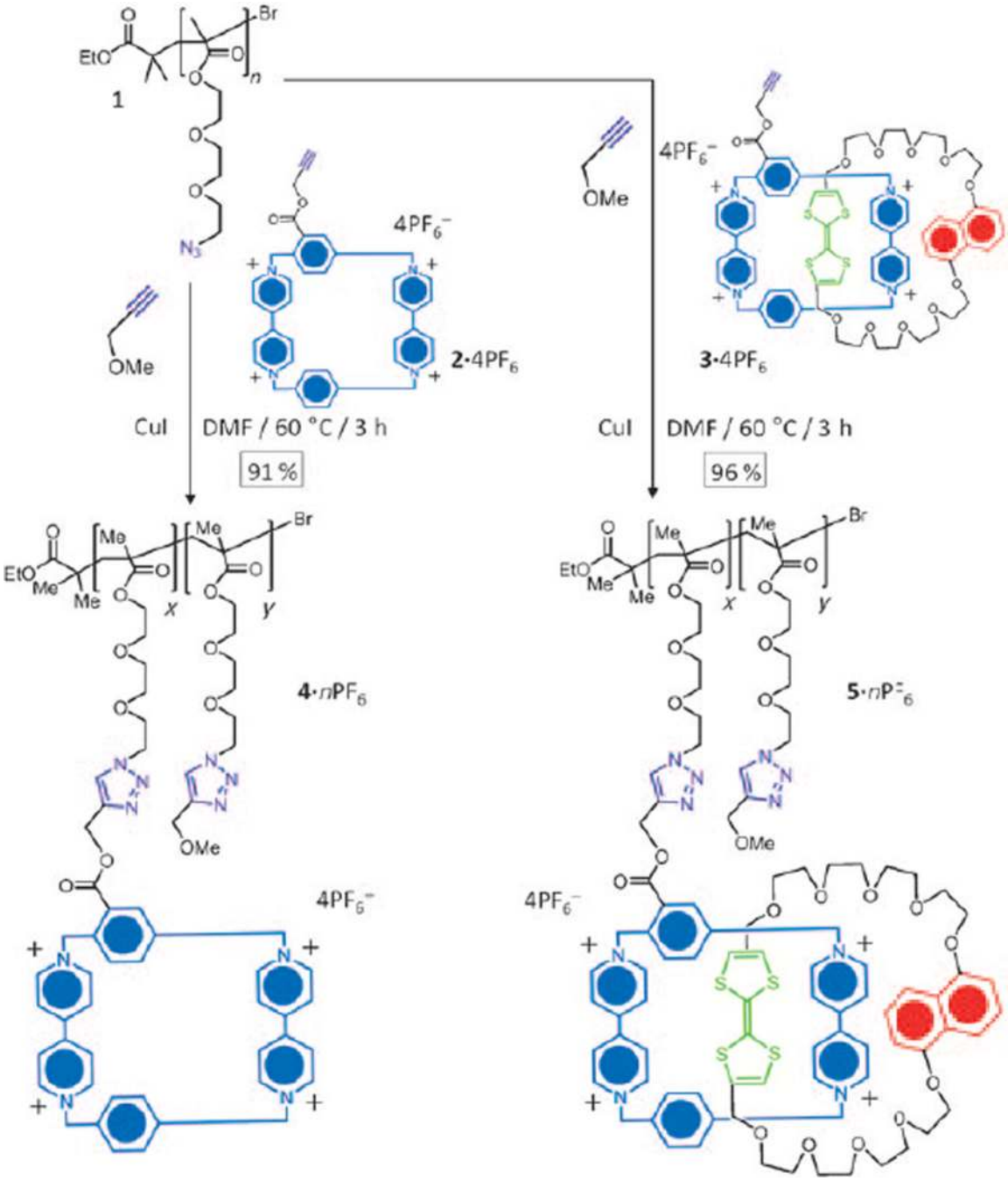

Scheme 1.

Click functionalization of polymer **1** (n = 160) with the alkyne-functionalized tetracationic cyclophane **2**·4PF_6 and the alkyne-functionalized bistable [2]catenane **3**·4PF_6 for the formation of **4**·$n$$PF_6$ (x = 27, y = 133) and **5**·$n$$PF_6$ (x = 42, y = 118).

Table 1

Ground-state equilibrium thermodynamic parameters ($\Delta H°$, $\Delta S°$, ΔG°_{298K}) and switching kinetics (τ_{298K}, k_{298K}, $\Delta G^{\ddagger}$) obtained after analysis of variable-temperature UV/Vis and variable-scan rate cyclic voltammetry experiments.

Species	$\Delta H°$ [a] [k cal mol^{-1}]	$\Delta S°$ [b] [cal mol^{-1} K^{-1}]	ΔG°_{298K} [c] [kcal mol^{-1}]	τ_{298K} [d] [s]	k_{298K} [d] [s^{-1}]	$\Delta G^{\ddagger}_{298K}$ [d] [kcal mol^{-1}]
3·4PF$_6$	3.9(±0.1)	7.9(±0.2)	1.5(±0.2)	1.9(±0.9)	0.52(±0.24)	17.8(±5.0)
5·*n*PF$_6$[e]	3.8(±0.1)	7.5(±0.1)	1.6(±0.1)	0.9(±0.1)	1.11(±0 .07)	17.4(±0.5)

[a] Obtained from a linear Van't Hoff plot where the slope of the line is equal to $-\Delta H°/R$.

[b] Obtained from a linear Van't Hoff plot where the intercept is equal to $\Delta S°/R$.

[c] Calculated from the Gibbs free energy $\Delta G° = \Delta H° - T\Delta S°$.

[d] Kinetic data obtained from 3 mm samples in DMF (0.1M TBAPF$_6$), with a glassy carbon working electrode, at various scan rates versus Ag/AgCl.

Angew Chem Int Ed Engl. Author manuscript; available in PMC 2014 February 20.